UV-Visible Technique for Studying Powder Coatings and Their Dissolution

Önder Pekcan—Istanbul Technical University*
Ertan Arda—Trakya University†

UV-Visible (UVV) technique was used to monitor powder coating and its dissolution processes from hard latex particles. Three sets of latex coatings were prepared from poly(methyl methacrylate) (PMMA) particles. The first set of coatings was annealed at elevated temperatures in various time intervals during which reflected photon intensity, I_{rf}, was measured. The second set of coatings was annealed at various temperatures in 10 min time intervals during which transmitted intensity, I_{tr}, was measured. I_{rf} first decreased and then increased as the annealing temperature was increased. Decrease in I_{rf} was explained with the void closure mechanism due to viscous flow. Increase in I_{tr} and I_{rf} against time and temperature were attributed to an increase in crossing density at the junction surface. The activation energy of viscous flow, ΔH, was measured and found to be around 8 kcal/mol and the back and forth activation energies (ΔE_{rf} and ΔE_{tr}) were measured and found to be around 49 and 53 kcal/mol for a reptating polymer chain across the junction surface. Diffusion of solvent molecules (chloroform) into the annealed latex coatings was followed by desorption of PMMA chains for the third set of films. Desorption of pyrene, P, labeled PMMA chains was monitored in real-time by the absorbance change of pyrene in the polymer-solvent mixture. A diffusion model with a moving boundary was employed to quantify real-time UVV data. Diffusion coefficients of desorbed PMMA chains were measured and found to be between 2 and 0.6 $\times 10^{-11}$ cm^2 s^{-1} in the 100 and 275°C temperature range.

INTRODUCTION

Latex coatings are generally formed by coalescence of submicron polymer particles in the form of a colloidal dispersion, usually in water. The term "latex film" normally refers to a film formed from soft latex particles (glass transition temperature (T_g) below room temperature) where the forces accompanying the evaporation of water are sufficient to compress and deform the particles into transparent, void-free film. However, latex coatings can also be obtained by compression molding of a film of dried latex powder composed of relatively hard polymers such as polystyrene (PS) or poly(methyl methacrylate) (PMMA) that have T_g above room temperature. Hard latex particles remain essentially discrete and undeformed during drying. The mechanical properties of such coatings can be evolved after all the solvent has evaporated by an annealing process which first leads to void closure and then interdiffusion of chains across particle-particle interfaces. After the void closure process is completed, the mechanism of coating formation, by annealing of hard latex films known as interdiffusion of polymer chains is followed by healing at the polymer-polymer interface. In general, when two identical polymeric materials are brought into intimate contact and heated at a temperature above the glass transition temperature the polymer chains become mobile, and interdiffusion of polymer chains across the interface can occur. After this process the junction surface becomes indistinguishable in all respects from any other surface that might be located in the polymeric material. This process is called healing of the junction at which the joint achieves the same cohesive strength as the bulk polymeric material. The word interdiffusion in polymer science is used for the process of mixing, intermingling, and homogenization at the molecular level, which implies diffusion among polymer chains.

In the bulk state, polymer chains have a Gaussian distribution of segments. Chains confined to the half-space adjacent to the junction have distorted conformations.[1,2] Diffusion across the junction leads to configura-

Presented at the 2000 Spring Meeting of the PMSE Div. of the American Chemical Society, March 26-30, 2000, San Francisco, CA.
*Dept. of Physics, Maslak 80626 Istanbul, Turkey.
†Dept. of Physics, 22030 Edirne, Turkey.

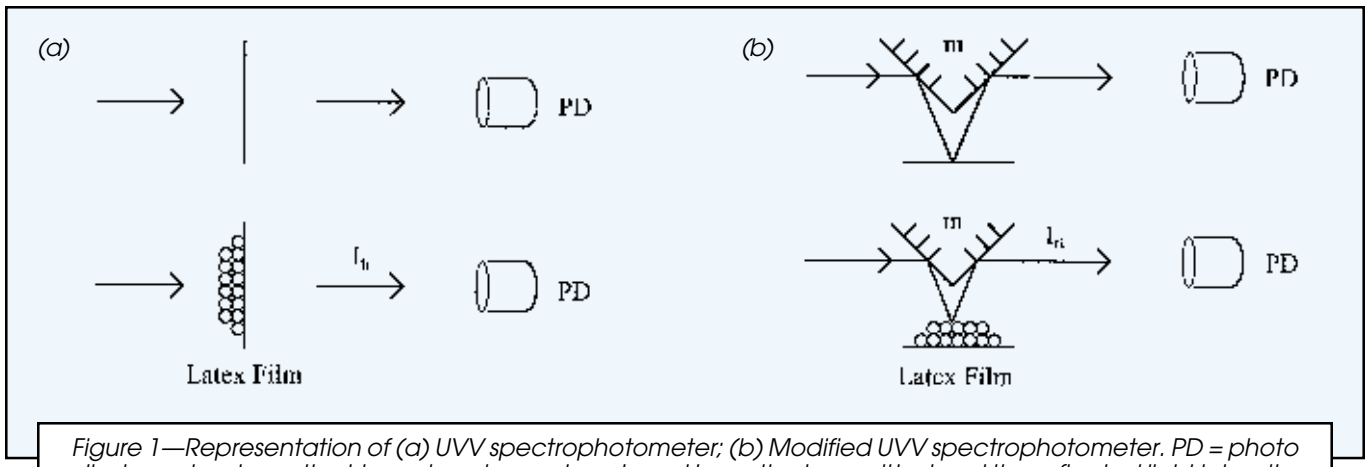

Figure 1—Representation of (a) UVV spectrophotometer; (b) Modified UVV spectrophotometer. PD = photo diode and m shows the triangular mirror system. I_{tr} and I_{rf} are the transmitted and the reflected light intensity.

tional relaxation and recovery of Gaussian chain behavior. Polymers much larger than a certain length are often pictured as confined to a tube, and diffusion occurs by reptile-like motion.[1] In this model each polymer chain is considered to be confined to a tube along the length of which it executes a random back and forth motion. This reptile-like motion will cause the chain to slip out of a section of tube at one end or the other. The reptation time, T_R, describes the time necessary for a polymer to diffuse a sufficient distance for all memory of the initial tube to be lost. This is the time it takes for initial configuration to be forgotten and the first relaxation to be completed.

Transmission electron microscopy (TEM) has been the most common technique used to investigate the structure of dried films.[3] Patterns of hexagons, consistent with face centered cubic packing, are usually observed in highly ordered films. When these films are annealed, complete disappearance of structure is sometimes observed, which is consistent with extensive polymer interdiffusion. Freeze fracture TEM (FFTEM) has been used to study the structure of dried latex films.[4,5] Small-angle neutron scattering (SANS) has been used to study latex film formation at the molecular level. Extensive studies using SANS have been performed by Sperling and co-workers[6] on compression molded PS films. Direct-nonradiative energy transfer (DET) method has been employed to investigate the film formation processes from dye labeled hard[7] and soft[8,9] polymeric particles. The steady state fluorescence (SSF) technique combined with DET has been used to examine healing and interdiffusion processes in dye labeled hard latex systems.[10-12] Recently we have reported photon transmission studies for powder coating from polystyrene particles.[13,14]

The polymer dissolution process is very different from, and more complicated than, small molecule dissolution. The dissolution of small molecules can be explained by simple diffusion laws[15] and a unique diffusion rate. However, polymeric material dissolve mainly in three different stages: solvent penetration, polymer relaxation, and diffusion of polymer chains into the solvent reservoir. In the first stage, the penetration distance of solvent molecules mainly depends on free volume, which in turn depends on the flexibility of the chains, backbone, and side groups, as well as the thermal history of the polymer. These first solvent molecules act as a plasticizer, and, as a result, these regions of the polymer start to swell. In the second stage, a gel layer is created by the relaxing polymer chains. This transition layer is composed of both polymer chains and solvent molecules. If the solvent-polymer interactions are more dominant than the polymer-polymer interactions, maximum swelling is obtained. This is the case when a good solvent is used during dissolution of a polymer material. In the last stage, chain disentanglement takes place, then chains separate from the bulk and diffuse into the solvent.

Poly(methyl methacrylate) film dissolution was studied using laser interferometry by varying the molecular weight and solvent quality.[16] Limm et al.[17] modified the interferometric technique and studied the dissolution of fluorescence labeled PMMA films. By monitoring the intensity of fluorescence from the film along with the interferometric signal, the solvent penetration rate into the film and the dissolution are measured simultaneously. A real time, nondestructive method for monitoring small molecule diffusion in polymer films was developed.[18,19] This method is essentially based on the detection of excited fluorescence dyes desorbing from a polymer film into a solution in which the film is placed. We have reported a steady state fluorescence (SSF) study on the dissolution of both annealed latex film and PMMA discs using real-time monitoring of fluorescence probes.[20-22] Recently, fast transient fluorescence (FTRF) technique was used to study dissolution of polymer glasses.[23]

In this work, evolution in transparency of two different sets of powder coatings formed from hard latex particles

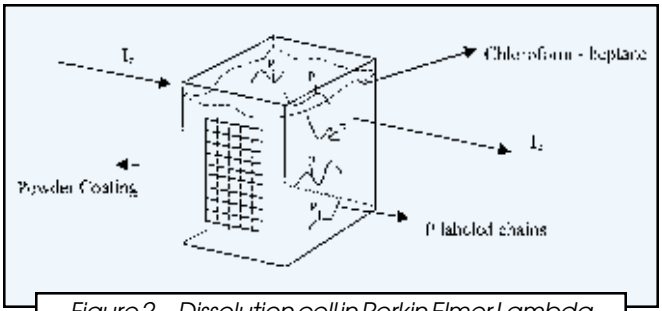

Figure 2—Dissolution cell in Perkin Elmer Lambda 2S spectrophotometer.

was studied by measuring the transmitted, I_{tr}, and the reflected, I_{rf}, photon intensities. It was shown that the variation in transparency is related to the variation in I_{tr} and I_{rf} intensities. The first set of coatings was annealed in equal time intervals at elevated temperatures above the T_g of PMMA, and I_{rf} intensities were measured by a modified UV-Visible (UVV) spectrophotometer. The second set of coatings was isothermally annealed in equal time intervals above T_g, and the increases in I_{tr} intensities were measured with a nonmodified UVV spectrophotometer. Decreases and increases in I_{rf} were explained by the increase in void closure and crossing density respectively by increasing annealing temperature during coating. The increase in I_{tr} in the second set of experiments, by increasing the annealing time, was also attributed to an increase in the crossing density. The method developed by Prager and Tirrell (PT)[1] was employed to investigate the healing processes at the junction surface. Increases in I_{tr} and I_{rf} intensities, with respect to annealing time and temperature, were used to measure the activation energies of back and forth motion for the reptating polymer chain across the polymer-polymer interface.

Chloroform-heptane mixture was used as a dissolution agent. UVV experiments were performed for real-time monitoring of the dissolution processes. The dissolution experiments were designed so that pyrene, P, labeled PMMA chains desorbing from swollen gel were detected by the UV absorption of P. Moving boundary model,[15] which was used to understand the diffusion in two distinct regions separated by a moving interface, was employed to interpret the UVV data.

EXPERIMENTAL

In UVV experiments, hard latex particles having two components were used[24,25]; the major part, PMMA, comprises 96 mol% of the material and the minor component, poly(iso butylene) (PIB) (4 mol%), forms an interpenetrating network through the particle interior[26,27] very soluble in certain hydrocarbon media. A thin layer of PIB covers the particle surface and provides colloidal stability by steric stabilization. PMMA-PIB polymer particles were prepared separately in a two-step process in which MMA in the first step was polymerized to low conversion in cyclohexane in the presence of PIB containing 2% isoprene units to promote grafting. The graft copolymer so produced served as a dispersant in the second stage of polymerization, in which MMA was polymerized in a cyclohexane solution of the polymer. Details have been published.[28] A stable dispersion of the polymer particles was produced, ranging in radius from 1 to 3 μm. Molecular weight of the polymer particle was measured by gel permeation chromatography (GPC) and found to be 1.1×10^5 with the polydispersity of 2.33. Spherical particle sizes were measured from electron micrographs of particles. A combination of ^{1}H-NMR and UV analysis indicated that these particles contain 4 mol% PIB. PMMA chains were labeled with pyrene dyes for dissolution experiments. (These particles were prepared by B. Williamson in Prof. M.A. Winnik's laboratory in Toronto). Two different sets of experiments were prepared from the particles by dispersing PMMA-PIB latex in heptane in a test tube with the solid content taken to be as 1%. Films were prepared from the dispersion of particles by placing the same number of drops on glass plates with the size of 0.9×3.2 cm^2 and allowing the heptane to evaporate. Here we were careful that the liquid dispersion from droplets covered the whole surface area of the plate and remained there until the heptane evaporated. Samples were weighed before and after the film casting to determine the film thicknesses. Average size for the particles was taken to be 2 μm to calculate the number of layers in the films. Glass plates were cleaned with acetone after they were used.

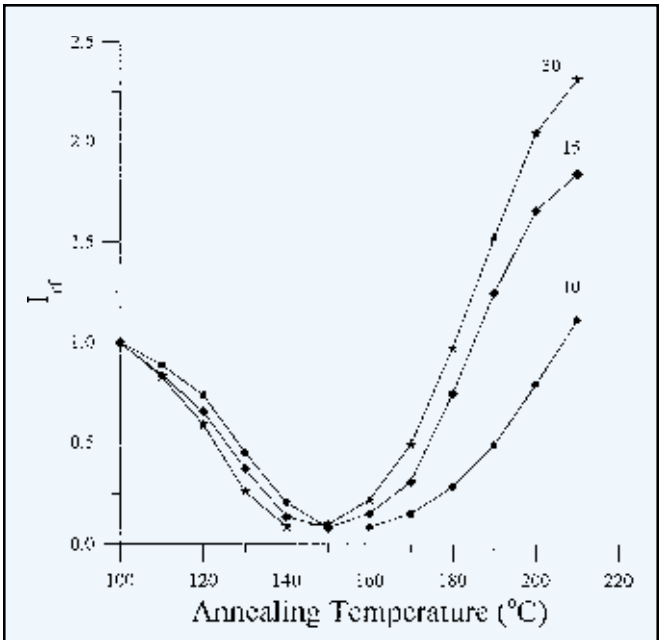

Figure 3—Plot of reflected photon intensity I_{rf} versus annealing temperature. Numbers on each curves indicate the annealing time intervals (min).

In this work the first set of UVV experiments was carried out to measure I_{rf} from the annealed powder coatings. Annealing process of the latex films was performed in an oven in air above T_g of PMMA after evaporation of heptane, in 30, 15, and 10 min intervals at elevated temperatures between 110 and 210°C. The temperature was maintained within ± 1°C during annealing. After annealing, each sample was placed in the model Lambda 2S UV-Visible spectrophotometer of Perkin Elmer. I_{rf} from coatings were detected between 300-400 nm. Another glass plate was used as a standard for all UVV experiments. In order to measure the reflected intensity, I_{rf}, from coatings, UVV spectrophotometer is slightly modified as presented in *Figure* 1b where two mirrors were placed in triangular position on the path of the light beam, which hits the surface of the coating to produce I_{rf} intensity. *Figure* 1a presents the normal UVV spectrophotometer for comparison, which measures the transmitted intensity, I_{tr}, from the coating.

In the second set of UVV experiments, the annealing process of the powder coatings was performed in air above T_g of PMMA after evaporation of heptane, in 10 min intervals at elevated temperatures between 160-190°C. The tem-

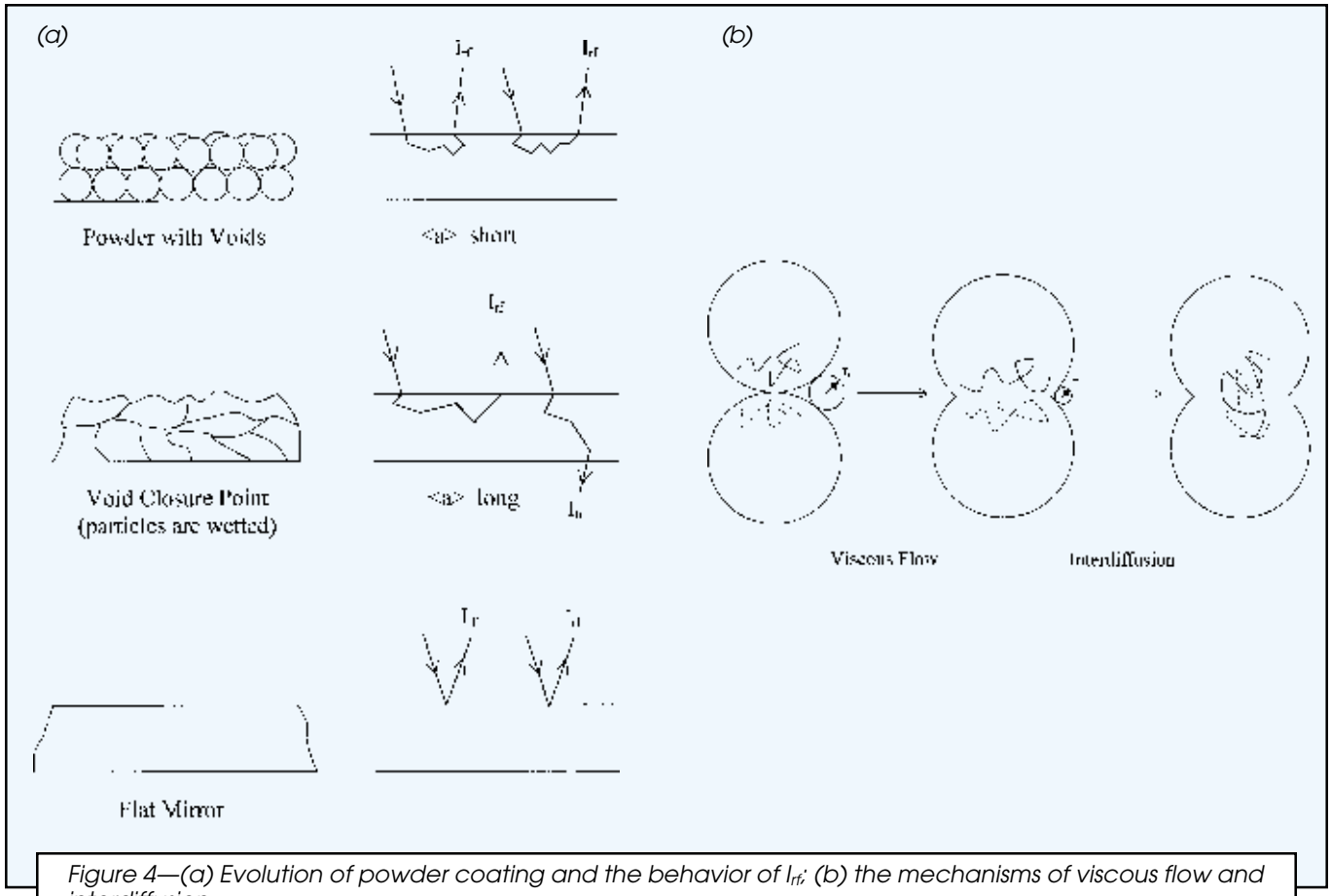

Figure 4—(a) Evolution of powder coating and the behavior of I_{rf}; (b) the mechanisms of viscous flow and interdiffusion.

perature was maintained within ±1°C during annealing. After annealing, each sample was placed in the UVV spectrophotometer and I_{tr} intensities were detected between 300-400 nm. Another glass plate was used as a standard for all UVV experiments as shown in *Figure* 1a. All measurements were carried out at room temperature after the annealing processes were completed.

Dissolution experiments were performed in a $1.0 \times 1.0 \times 4.5$ cm^3 quartz cell. Coating samples were attached at one side of a UV quartz cell filled with chloroform-heptane mixture. The cell was placed in the spectrophotometer and then illuminated with 345 nm excitation light which is strongly absorbed by pyrene. P absorbance (A_p), which is proportional to the number of P labeled chains in a polymer-solvent solution change in the UV cell was monitored as a function of time during the dissolution process using the "time drive" mode of the spectrophotometer. The dissolution cell and the coating position are presented in *Figure* 2. In dissolution experiments, coating samples were dissolved in (90+10%) chloroform-heptane mixture. All UVV measurements were carried out at room temperature.

RESULTS AND DISCUSSION

Reflected photon intensities, I_{rf}, from coating samples were obtained by using the modified UVV spectrophotometer and are plotted versus annealing temperature for 30, 15, and 10 min intervals in *Figure* 3. It is seen that all I_{rf} curves first decreased by showing a minimum then increased to larger values at each annealing time interval. Initial decrease in I_{rf} is attributed to the void closure process. In other words, polymeric material flows to fill up the voids between particles and as a result coating reflects less photon. However, when annealing the coating above 160°C reflected photon intensity starts to increase and more photons can reach the photo diode as the interfaces start to heal and disappear. This picture can be visualized by taking into account the photon's mean free path <a> which is very short at the beginning of powder coating where many interparticle voids exist. At this stage coating reflects more photons; however, as the latex is annealed, interparticle voids start to disappear and <a> increases; as a result I_{rf} starts to decrease. Finally, when all the voids have disappeared, I_{rf} reaches the minima at 160°C where <a> becomes maximum.[29] Above 160°C, after all the voids have disappeared and complete wetting is reached, the coating gradually becomes a flat mirror. In other words, as the polymer chains interdiffuse the coating surface starts to level off the quality of the mirror improves, and the coating reflects more photons, resulting in an increase in I_{rf}. All these pictures are summarized in *Figures* 4a and b where the evolution of powder coating and its mechanisms are presented, respectively. Here it has to be noted that because of the geometry of the light beam, reflected light primarily measures the surface quality of the coating; however, trans-

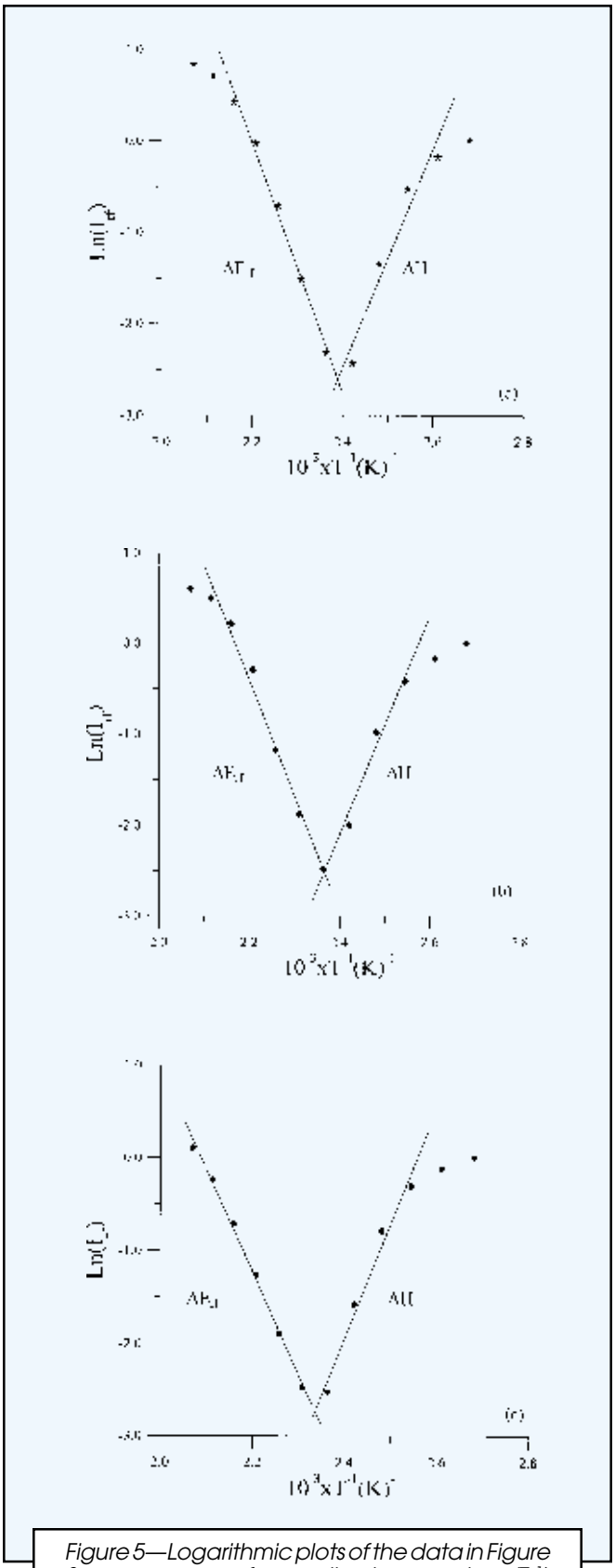

Figure 5—Logarithmic plots of the data in Figure 3 versus reverse of annealing temperature (T^{-1}) for (a) 30, (b) 15, (c) 10 min time intervals.

mitted light, which hits the coating at a 90° angle, detects the quality of the whole material (see *Figure* 1).

Void Closure Kinetics

To quantify the behavior of I_{rf} below its minima, we introduce the phenomenological void closure model. The void closure kinetics can determine the time for optical transparency and latex film formation.[30] To relate the shrinkage of spherical void of radius, r, to the viscosity of surrounding medium, η, an expression was derived and given by the following relation.[30]

$$\frac{dr}{dt} = -\frac{\gamma}{2\eta}\left(\frac{1}{\rho(r)}\right) \tag{1}$$

where γ is surface energy, t is time and ρ(r) is the relative density. It has to be noted that here surface energy causes a decrease in void size and the term ρ(r) varies with the microstructural characteristics of the material, such as the number of voids, the initial particle size, and packing. Equation (1) is similar to one which was used to explain the time dependence of the minimum film formation temperature during latex film formation.[24,30] If the viscosity is constant in time, integration of equation (1) gives the relation as

$$t = -\frac{2\eta}{\gamma}\int_{r_o}^{r}\rho(r)dr \tag{2}$$

where r_o is the initial void radius at time t=0 (see *Figure* 4b).

The dependence of the viscosity of polymer melt on temperature is affected by the overcoming of the forces of macromolecular interaction which enables the segments of the polymer chain to jump over from one equilibration position to another. This process happens at temperatures at which free volume becomes great enough and is connected with the overcoming of the potential barrier. The height of this barrier can be characterized by free energy of activation, ΔG, during viscous flow. Frenkel-Eyring[24-25] theory produces the following relation for the temperature dependence of viscosity

$$\eta = \frac{N_o h}{V}\exp(\Delta G/kT) \tag{3}$$

where N_o is Avagadro's number, h is Planck's constant, V is molar volume and k is Boltzmann constant. It is known that ΔG = ΔH–TΔS, then equation (3) can be written as

$$\eta = A\exp(\Delta H/kT) \tag{4}$$

where ΔH is the activation energy of viscous flow, i.e., the amount of heat which must be given to one mole of mate-

Table 1—Experimentally Measured Activation Energies of Void Closure (ΔH) and Back and Forth Motion of Chains (ΔE_{rf}) for Various Annealing Times

Annealing time interval (min)	30	15	10	
ΔE_{rf} (kcal/mol)	54.3	50.4	43.9	49.5
ΔH (kcal/mol)	7.9	7.9	8.2	8.0

ΔH and ΔE_{rf} values obtained by fitting the data in *Figure* 3 to equation (9) and equation (14) respectively. The last column gives the averaged values of activation energies.

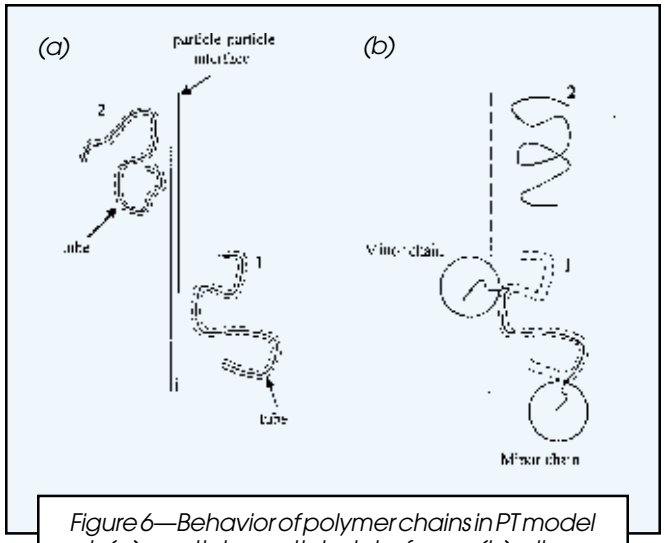

Figure 6—Behavior of polymer chains in PT model at (a) particle-particle interface, (b) disappeared interface. Dotted lines represent the tube created by the topological constraints imposed by the neighboring chains. 1 shows a chain still retaining some portion in its initial tube and 2 represents a chain relaxed at least once.

rial for creating the act of a jump during viscous flow. ΔS is the entropy of activation of viscous flow. Here A represents a constant for the related parameters. Combining equations (2) and (4), the following useful equation is obtained

$$t = -\frac{2A}{\gamma}\exp\left(\frac{\Delta H}{kT}\right)\int_{r_o}^{r}\rho(r)dr \qquad (5)$$

Equation (5) will be employed to interpret the data of photon reflection to explain the void closure mechanism.

To quantify the behavior of I_{rf} below void closure point (t_c,T_c), equation (5) can be employed by assuming that the interparticle voids are in equal size and the number of voids stays constant during film formation (i.e., $\rho(r) \propto r^{-3}$), then integration of equation (5) gives the relation

$$t = \frac{2AC}{\gamma}\exp\left(\frac{\Delta H}{kT}\right)\left(\frac{1}{r^2} - \frac{1}{r_o^2}\right) \qquad (6)$$

where C is a constant related to relative density ρ(r). It is well known that scattering intensity increases with volume squared (the 6th power radius) of scattering object. If the assumption is made that I_{rf} is proportional to the 6th power of void radius, r, then equation (6) can be written as

$$t = \frac{2AC}{\gamma}\exp\left(\frac{\Delta H}{kT}\right)I_{rf}^{-1/3} \qquad (7)$$

Here r_o^{-2} is omitted from the relation since it is very small compared to r^{-2} values after void closure processes start. Equation (7) can be solved for I_{rf} to interpret the results in *Figure* 3 as

$$I_{rf}(T) = S(t)\exp\left(\frac{3\Delta H}{kT}\right) \qquad (8)$$

where $S(t) = (2AC/\gamma t)^3$. For a given time the logarithmic form of equation (8) can be written as follows

$$\ln I_{rf}(T) = \ln S(t) + \frac{3\Delta H}{kT} \qquad (9)$$

Below the minima data in *Figure* 3 are fitted to equation (9) and ΔH values are obtained from the slopes of the straight lines in *Figure* 5. ΔH values are listed in *Table* 1 for various time intervals. The averaged ΔH value is found to be 8 kcal/mol which is quite close to the values for carbon chain polymers given in the literature.[25] The activation

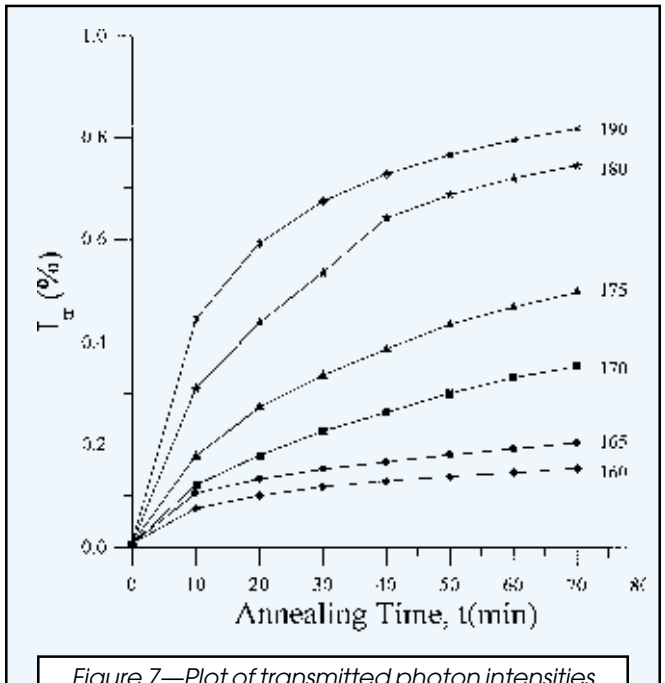

Figure 7—Plot of transmitted photon intensities (I_{tr}) versus annealing time at temperatures given on each curve in (°C) for coatings.

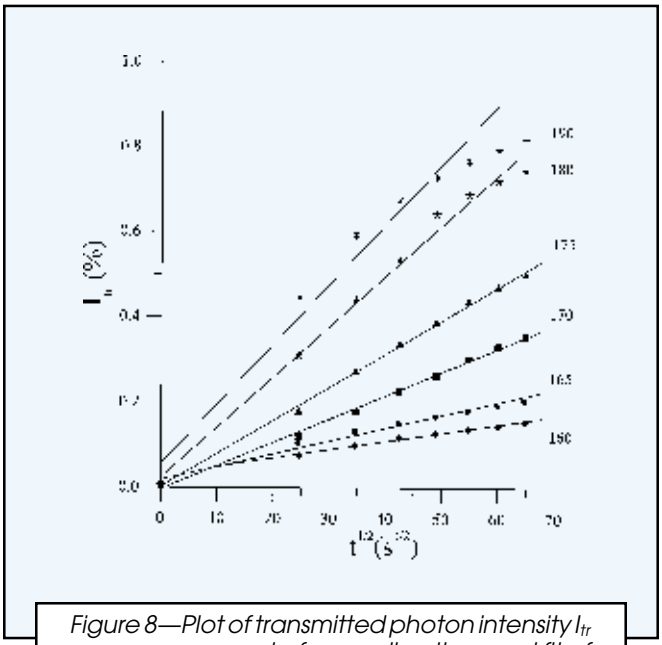

Figure 8—Plot of transmitted photon intensity I_{tr} versus square root of annealing time and fit of the data to equation (16), for various temperatures for coatings. Numbers on each curve present the annealing temperatures (°C).

energy of viscous flow, i.e., the dependence of viscosity on temperature is determined by the structure of the polymer chain. In other words, the type of branches and the presence of polar groups in the chain determine the kinetic flexibility of the polymer. For carbon chain polymers ΔH are found to be 5 to 7 kcal/mol (polyethylene). ΔH reaches to the value of 15 kcal/mol for poly (iso butylene). For polystyrene whose side groups are phenyl rings ΔH rises to 28 kcal/mol. ΔH is much higher for polyvinyl chloride (35 kcal/mol) and polyvinyl acetate (60 kcal/mol) polymers. Here it has to be noted that curves in *Figure* 3 are used up to their minima, i.e., left hand side of void closure temperature, T_c. The right hand side of the curves in *Figure* 3 represents the interdiffusion processes during coating, which will be discussed in the next section.

Crossing Density at Junction Surface

When coating samples were annealed at elevated temperatures in equal time intervals, a continuous increase in I_{rf} intensities above 160°C was observed (see *Figure* 3). The increase in I_{rf} was already explained in the previous section, by leveling of the coating due to disappearance of particle-particle interfaces. As the annealing temperature is increased, some part of the polymer chains may cross the junction surface and the particle boundaries start to disappear. As a result, the reflected photon intensities increase due to the creation of high quality, transparent mirror film.

To quantify these results, the Prager-Tirrell (PT) model[1] for the chain crossing density was employed. These authors used de Gennes's "reptation" model to explain configurational relaxation at the polymer-polymer junction where each polymer chain is considered to be confined to a tube in which executes a random back and forth motion. A homopolymer chain with N freely jointed segments of length L was considered by PT, which moves back and forth by one segment with a frequency, ν. In time the chain displaces down the tube by a number of segments, m. Here, $\nu/2$ is called the "diffusion coefficient" of m in one-dimensional motion. PT calculated the probability of the net displacement with m during time, t, in the range of $n - \Delta$ to $n - (\Delta + d\Delta)$ segments. A Gaussian probability density was obtained for small times and large N. The total "crossing density," $\sigma(t)$, (chains per unit area) at the junction surface was then calculated from the contributions σ_1 (t) due to chains still retaining some portion of their initial tubes, plus a remainder, σ_2 (t). Here the σ_2 (t) contribution comes from chains which have relaxed at least once. *Figure* 6 shows the pictorial representation of the σ_1 and σ_2 contributions at the particle-particle boundary before and after the disappearance of the interface. Here the small segments present the part of the polymer chain called minor chain. In terms of reduced time, $\tau = 2\nu t/N^2$, the total crossing density can be written as

$$\sigma(\tau)/\sigma(\infty) = 2\pi^{-1/2}\left[\tau^{1/2} + 2\sum_{k=0}^{\infty}(-1)^n\left[\tau^{1/2}\exp(-k^2/\tau) - \pi^{-1/2}erfc(k/\tau^{1/2})\right]\right] \quad (10)$$

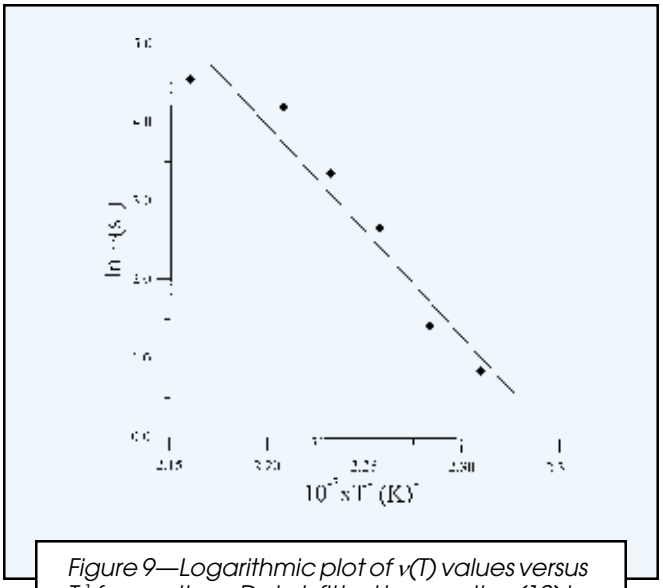

Figure 9—Logarithmic plot of $\nu(T)$ values versus T^{-1} for coatings. Data is fitted to equation (12) to produce ΔE values.

For small τ values the summation term of equation (10) is very small and can be neglected, which then results in

$$\sigma(\tau)/\sigma(\infty) = 2\pi^{-1/2}\tau^{1/2} \quad (11)$$

This was predicted by de Gennes on the basis of scaling arguments. In order to compare our results with the crossing density of the PT model, the temperature dependence of $\sigma(\tau)/\sigma(\infty)$ can be modeled by taking into account the following Arrhenius relation for the linear diffusion coefficient

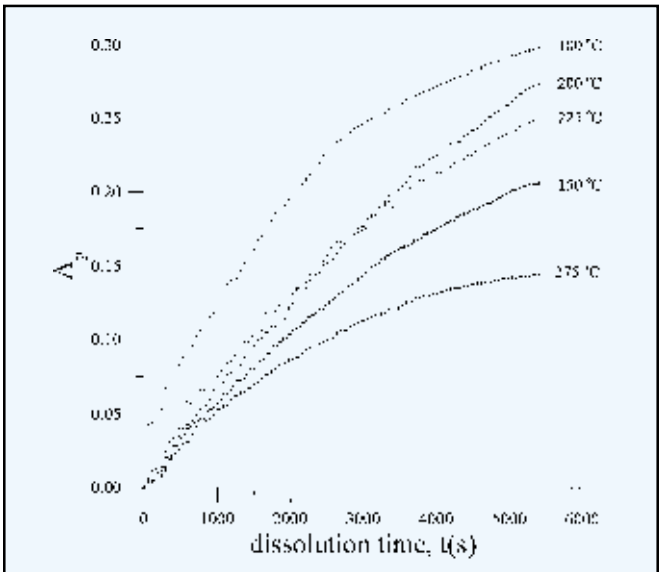

Figure 10—P absorbance, A_p, versus dissolution time. Numbers on each curve indicate the annealing temperature of coatings. The cell was illuminated at 345 nm during dissolution experiment.

$$\nu = \nu_o \exp(-\Delta E/kT) \quad (12)$$

Here ΔE is defined as the activation energy for the back and forth motions. By combining equations (11) and (12), a useful relation is obtained

$$\sigma(\tau)/\sigma(\infty) = R_o \exp(-\Delta E/2kT) \quad (13)$$

where $R_o=(8\nu_o t/\pi N^2)^{1/2}$ is a temperature independent coefficient.

The increase in I_{rf} is already related to the disappearance of particle-particle interfaces, i.e., as annealing temperature is increased, more chains relaxed across the junction surface and as a result the crossing density increased. Now, it can be assumed that I_{rf} is proportional to the crossing density σ(T) and then the phenomenological equation can be written as

$$I_{rf}(T)/I_{rf}(\infty) = R_o \exp(-\Delta E_{rf}/2kT) \quad (14)$$

Logarithmic plots of I_{rf} versus T^{-1} are presented on the left side of *Figures* 5a, b, and c for films 30, 15, and 10 min annealing time intervals. The activation energies, ΔE_{rf} are produced by fitting the data to equation (14) and the averaged value is found to be as 49.5 kcal/mol. The measured ΔE_{rf} values are listed in *Table* 1.

Transmitted photon intensities from coatings are obtained and plotted versus annealing time in *Figure* 7 at various temperatures. It is seen that I_{tr} intensity curves all present an increase as annealing time is increased. This behavior of I_{tr} suggests that powder coatings become more transparent to photons as they are annealed for longer times. Lower intensities observed from coatings annealed at lower temperatures, by indicating that photons cannot be transmitted as well as they are from coatings annealed at high temperatures. In other words, some photons dissipate or cannot reach the photomultiplier tube after they pass through the coatings annealed at low temperatures. Increasing the annealing temperature I_{tr} presents greater values as the annealing time is increased. This behavior of I_{tr} intuitively predicts that annealing the coatings in longer times and higher temperatures creates more transparent coating. All I_{tr} curves reach a plateau at long annealing times.

When coating samples were annealed in elevated time intervals at various temperatures, a continuous increase in I_{tr} intensities was observed. The increase in I_{tr} can be explained by the increase in transparency of coating due to the disappearance of particle-particle interfaces. As the annealing time is increased some part of the polymer chains may cross the junction surface and particle boundaries start to disappear. As a result, the transmitted photon intensity I_{tr} increases, similar to the increase in I_{rf} which was explained in the previous section.

In order to quantify these results, the Prager-Tirrell (PT) model[1] for the chain crossing density can be employed. Now equation (13) can be written in time dependent form as follows

$$\sigma(\tau)/\sigma(\infty) = R_1 \exp(-\Delta E/2kT)t^{1/2} \quad (15)$$

where $R_1 = (8/\pi N^2)^{1/2}$ is a temperature and time independent coefficient.

The increase in I_{tr} is already related to the disappearance of particle-particle interfaces, i.e., as annealing time is increased, more chains relaxed across the junction surface and as a result the crossing density increased. Now it can be assumed that I_{tr} is proportional to σ(t) and then the phenomenological equation can be written as

$$I_{tr}(t)/I_{tr}(\infty) = R_1 \exp(-\Delta E/2kT)t^{1/2} \quad (16)$$

In *Figure* 8, I_{tr} values are plotted against $t^{1/2}$ for latex films annealed at various temperatures. I_{tr} increases linearly for all samples, which indicates that the model chosen for the disappearance of particle-particle interfaces works well for our data. The slopes of the curves in *Figure* 8 produce temperature dependent ν(T) values. The logarithmic plots of ν(T) versus T^{-1} is shown in *Figure* 9 which also presents a nice linear relation, indicating that the PT

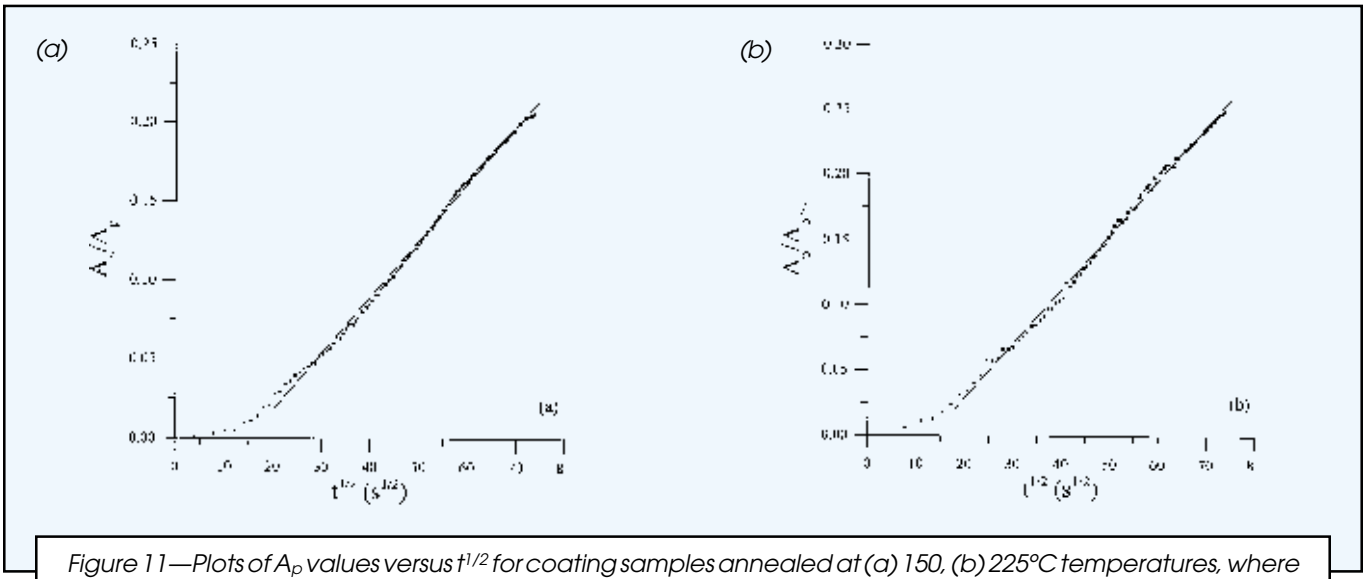

Figure 11—Plots of A_p values versus $t^{1/2}$ for coating samples annealed at (a) 150, (b) 225°C temperatures, where t is the dissolution time. Data is fitted to equation (18) to produce D_1 values.

Table 2—Desorbing Diffusion Coefficients Obtained by Fitting the Data in *Figure* 9 to Equation (18) at Various Temperatures

Annealing temperature (°C)	100	125	150	175	200	225	250	275
$D_1 \times 10^{-11}$ ($cm^2\ s^{-1}$)	1.76	1.06	0.90	2.10	1.88	1.25	1.42	0.60

model used fits our data quite well. The back and forth activation energies, ΔE, are produced by fitting the data to equation (12). The averaged value is found to be 53 kcal/mol.

Film Dissolution and Moving Boundary Model

Labeled pyrenes in polymer-solvent mixture in the UV cell were excited at 345 nm during dissolution experiments and the variation in absorbance (A_p) was monitored with the time drive mode of the spectrophotometer. P absorbance, A_p, is plotted in *Figure 10* as a function of "dissolution time" for the latex samples annealed at 100, 150, 200, 225, and 275°C temperatures. It can be seen that as the dissolution time increases, a continuous increase in A_p is observed for all coating samples. Here it is interesting to note that the coating annealed at 100°C dissolved faster than the coating annealed at 275°C.

Various mechanism and mathematical models were considered for the polymer dissolution. Tu and Quano[31] proposed a model that includes polymer diffusion in a liquid layer adjacent to the polymer and moving out of the liquid-polymer boundary. The key parameter for this model was the polymer disassociation rate, defined as the rate at which polymer chains desorb from the gel interface. Lee and Peppas[32] extended this model for films to express the polymer dissolution rate where gel thickness was found to be proportion to $(\text{time})^{1/2}$. A relaxation controlled model was proposed by Brochard and de Gennes[33] where, after a swelling gel layer was formed, desorption of polymer from the swollen bulk was governed by the relaxation rate of the polymer stress. This rate was found to be of the same order of magnitude as the reptation time. The dependence of the radius of gyration and the reptation time on polymer molecular weight and concentration were studied, using scaling law,[34] based on the reptation model.

In this paper we consider a model in which diffusion occurs in two distinct regions separated by a moving interface.[15] The moving interface can be marked by a discontinuous change in concentration, as in the absorption by a liquid of a single component from a mixture of gases or by a discontinuity in the gradient of concentration, as in the progressive freezing of a liquid. The motion of the interface relative to the two regions it separates may be caused by the disappearance of matter at the interface in one or both regions, which results in a bodily movement of the matter in one or both regions relative to the interface.

Discontinuities have been observed in several practical systems, for instance, when two metals interdiffuse.[15] The sharp advancing boundary is well known in many polymer-solvent systems, which is considered as a discontinuity for same purposes. When the diffusion coefficient is discontinuous at a concentration c, i.e., the diffusion coefficient is zero below c and constant and finite above c, then the total amount, M_t, of diffusing substance desorbed from unit area of a plane sheet of thickness, d, at time, t, is given by the following relation

$$\frac{M_t}{M_\infty} = 2\left(\frac{D_1}{\pi d^2}\right)^{1/2} t^{1/2} \qquad (17)$$

Where D_1 is the constant diffusion coefficient at concentration c_1. Here $M_\infty = c_1 d$ is the equilibrium value of M_t. If one assumes that the diffusion coefficient of polymer chains in coating is negligible in comparison to the desorbing coefficient, D_1, of polymer chains into solvent, then equation (17) can be written to employ our UVV data as follows

$$\frac{A_p}{A_{p\infty}} = 2\left(\frac{D_1}{\pi d^2}\right)^{1/2} t^{1/2} \qquad (18)$$

here it is assumed that M_t is proportional to A_p at time, t.

Plots of A_p versus $t^{1/2}$ are presented in *Figures* 11a and b for 150 and 225°C annealing temperatures, respectively. The desorption diffusion coefficients, D_1, are obtained from the linear fits in *Figure* 11 using equation (18) and are listed in *Table* 2. It is seen that D_1 values are independent of the annealing temperatures of the latex except at 275°C. The low value of D_1 (0.6×10^{-11} $cm^2\ s^{-1}$) at 275°C, compared to the average value of D_1 (1.5×10^{-11} $cm^2\ s^{-1}$), is attributed to a very high annealing temperature, where a mechanically strong coating is obtained which is quite difficult to be dissolved. The delay in dissolution at early times is seen in *Figures* 11a and b which can be explained with the polymer relaxation stage where a gel layer is created by the relaxing polymer chains; as a result no desorption has been shown yet. The observed D_1 values are consistent with our early findings, obtained using fluorescence technique.[20-22] When one compares the observed $D_1 \approx 10^{-11}$ $cm^2\ s^{-1}$ values with the backbone diffusion coefficient of the interdiffusing polymer chains during film formation from PMMA latex particles,[7,35] ($\approx 10^{-16}$ – 10^{-14}) 5-3 orders of magnitude difference can be seen. This is reasonable for the chains desorbing from swollen gel during dissolution of PMMA latex coatings.

SUMMARY

This paper introduces a UVV technique for monitoring powder coating and its dissolution processes. Reflected photon intensity, I_{rf}, was used to monitor viscous flow of polymeric material and the crossing density of the polymer chains at the particle-particle boundaries. Activation energies of viscous flow and back and forth motion of the backbone were measured and found to be 8 and 49 kcal/mol, respectively. Here it has to be noted that, since the size of particles range from 1 to 3μm, void distribution is not quite uniform which then results in nonuniform packing in the initial powder coating. On the other hand, SEM results show that average void diameter is at least four or five times smaller than the wavelength of the light used in

UVV experiments. These facts allow us to make the assumption used converting equation (6) to equation (7), however the assumption used to produce equation (6) is highly approximated. As a result we have to state that produced ΔH values are correct in some approximation. Transmitted photon intensity, I_{tr}, was used to measure back and forth frequencies of the reptating polymer chain which are found to be strongly dependent on the annealing temperature of the latex. These frequencies were used to calculate the activation energy of back and forth motion which is found to be 53 kcal/mol, in agreement with the previous findings in the experimental error range. Here it has to be emphasized that energy of viscous flow is found to be smaller than back and forth motion, i.e., the macroscopic behavior of polymeric material is much different energetically than the microscopic behavior.

In this work it is observed that dissolution of coatings obeys the Moving Boundary Model. The absorbance change of pyrene in the polymer-solvent mixture was monitored to measure the diffusion coefficients, D_1, of desorbed PMMA chains from the coating. D_1 values are found to be independent of the annealing temperature. Variation in D_1 values in *Table* 2 most likely shows the quality of coating surface. For example, high D_1 values of samples annealed at 100, 175, and 200ºC show that these coatings have higher surface area. However, lower D_1 values of samples annealed at 125, 150, and 275ºC came from lower surface area of these films. All these results show that the surface of these coatings forms quite arbitrarily, i.e., coating formation from hard latex particles is independent of annealing temperature.

In summary, UVV technique is found to be quite useful and simple to test the powder coating models at various stages. The dissolution model was also tested and very small diffusion coefficients were measured using the UVV technique.

References

(1) Prager, S. and Tirrell, M., "The Healing Process at Polymer-Polymer Interface," *J. Chem. Phys*., 75, 5194 (1981).
(2) Kim, Y.H. and Wool, R.P., "A Theory of Healing at a Polymer-Polymer Interface," *Macromolecules*, 16, 115 (1983).
(3) Vanderhoff, J.W., "Mechanism of Film Formation of Lattices," *Br. Polym. J*., 2, 161 (1970).
(4) Wang, Y., Kats, A., Juhue, D., Winnik, M.A., Shivers, R.R., and Dinsdale, C.J., "Freeze Fracture Studies of Latex Films Formed in the Absence and Presence of Surfactant," *Langmuir*, 8, 1435 (1992).
(5) Roulstone, B.J., Wilkinson, M.C., and Hearn, J., "Studies of Polymer Latex Films: II Effect of Surfactant on the Water Vapor Permeability of Polymer Latex Films," *Polym. Int*., 27, 43 (1992).
(6) Kim, K.D., Sperling, L.H., Klein, A., and Wignall, G.D., "Characterization of Film Formation from Direct Mini-Emulsified Polystyrene Latex Particles via SANS," *Macromolecules*, 26, 4624 (1993).
(7) Pekcan, Ö., Winnik, M.A., and Croucher, M.D., "Fluorescence Studies of Coalescence and Film Formation in PMMA Non-aqueous Dispersion Particles," *Macromolecules*, 23, 2673 (1990).
(8) Wang, Y., Zhao, C.L., and Winnik, M.A., "Molecular Diffusion and Latex Film Formation: An Analysis of Direct Non-Radiative Energy Transfer Experiment," *J. Chem. Phys*., 95, 2143 (1991).
(9) Wang, Y. and Winnik, M.A., "Energy Transfer Study of Polymer Diffusion in Melt-Pressed Films of Poly(methyl methacrylate)," *Macromolecules*, 26, 3147 (1993).
(10) Pekcan, Ö. and Canpolat, M., "Fluorescence Method of Studying Void Closure Kinetics During Film Formation from High-T Latex Particles," *J. Appl. Polym. Sci*., 66, 655 (1997).
(11) Canpolat, M. and Pekcan, Ö., "Photon Diffusion Study in Films Formed from High-T Latex Particles," *Polymer*, 36, 4433 (1995).
(12) Canpolat, M. and Pekcan, Ö., "Healing and Photon Diffusion during Sintering of High-T Latex Particles," *J. Polym. Sci. B, Polym. Phys*., 34, 691 (1996).
(13) Pekcan, Ö., Arda, E., Kesenci, K., and Piskin, E., "Photon Transmission Technique for Studying Film Formation from Polystyrene Latexes Prepared by Dispersion Polymerization Using Various Steric Stabilizers," *J. Appl. Polym. Sci*., 68, 1257 (1998).
(14) Arda, E., Bulmus, V., Piskin, E. and Pekcan, Ö., "Molecular Weight Effect on Latex Film Formation from Polystyrene Particles: A Photon Transmission Study," *J. Coll. Interface Sci*., 213, 160 (1999).
(15) Crank, J., *The Mathematics of Diffusion*, Clarendon Press, Oxford U.K., 1975.
(16) Krasicky, P.D., Groele, R.J., and Rodriguez, F., *J. Appl. Polym. Sci*., 35, 641 (1988).
(17) Limm, W., Dimnik, G.D., Stanton, D., Winnik, M.A., and Smith, B.A., *J. Appl. Polym. Sci*., 35, 2099 (1988).
(18) Krongauz, V.V., Mooney III, W.F., Palmer, J.W., and Patricia, J.J., "Real Time Monitoring of Diffusion in Polymer Film Using Fluorescence Tracer," *J. Appl. Polym. Sci*., 56, 1077 (1995).
(19) Krongauz, V.V. and Yohannan, R.M., *Polymer*, 31, 1130 (1990).
(20) Pekcan, Ö., Canpolat, M., and Kaya, D., "In situ Fluorescence Experiments for Real-Time Monitoring of Annealed High-T Latex Film Dissolution," *J. Appl. Polym. Sci.,* 60, 2105 (1996).
(21) Pekcan, Ö., Ugur, S., and Yilmaz, Y., "Real Time Monitoring of Swelling and Dissolution of Poly(methyl methacrylate) Discs Using Fluorescence Probes," *Polymer*, 38, 2183 (1997).
(22) Ugur, S. and Pekcan, Ö., "Determination of Relaxation and Diffusion Activation Energies During Dissolution of Latex Film Using in situ Fluorescence Technique," *Polymer*, 38, 5579 (1997).
(23) Ugur, S. and Pekcan, Ö., "Pyrene Lifetimes for Monitoring Polymer Dissolution: A Fast Transient Fluorescence Study," *Polymer*, 41, 1571 (2000).
(24) Mc Kenna, G.B., *In Comprehensive Polymer Science, Vol. 2*, Booth, C. and Price, C., (Eds.), Pergamon Press, Oxford U.K., 1989.
(25) Tager, A., *Physical Chemistry of Polymers*, MIR Publisher, Moscow, 1978.
(26) Pekcan, Ö., Winnik, M.A., and Croucher, M.D., "Direct Energy Transfer Studies on Doped and Labeled Polymer Latex Particles," *Phys. Rev. Lett*., 61, 641 (1988).
(27) Pekcan, Ö., "Inverted Klafter-Blumen Equation for Fractal Analysis in Particles with Interpenetrating Network Morphology," *Chem. Phys. Letter*, 20, 198 (1992).
(28) Winnik, M.A., Hua, M.H., Hongham, B., Williamson, B., and Croucher, M.D., *Macromolecules*, 17, 262 (1984).
(29) Canpolat, M. and Pekcan, Ö., "The Effect of Solid Content on Latex Coalescence and Film Formation: Steady-State Energy Transfer Study with Fluorescence Labeled Polymer," *J. Appl. Polym. Sci.*, 59, 1699 (1996).
(30) Keddie, J.L., Meredith, P., Jones, R.A.L., and Donald, A.M., *Film Formation in Waterborne Coatings*, Provder, T., Winnik, M.A., and Urban, M.W., (Eds.), ACS Symp. Ser. 648, pp. 332-348, Amer. Chem. Soc., 1996.
(31) Tu, Y.O. and Quano, A.C., *IBM J. Res. Dev*., 21, 131 (1977).
(32) Lee, P.I. and Peppas, N.A., *J. Controlled Release*, 6, 207 (1987).
(33) Brochardt, F. and de Gennes, P.G., *Phys. Chem. Hydrodynam*., 4, 313 (1983).
(34) Papanu, J.S., Soane, D.S., and Bell, A.T., *J. Appl. Polym. Sci*., 38, 859 (1989).
(35) Winnik, M.A., Pekcan, Ö., and Croucher, M.D., *Scientific Methods for the Study of Polymer Colloids and Their Applications*, Candau, F. and Ottewill, R.H., (Eds.), NATO, ASI, Kluwer, New York, 1988.